Black Holes as Neutrino Factories

Yifan Chen,[1, *] Xiao Xue,[2, 3, †] and Vitor Cardoso[1, 4, ‡]

[1] *Niels Bohr International Academy, Niels Bohr Institute, Blegdamsvej 17, 2100 Copenhagen, Denmark*
[2] *II. Institute of Theoretical Physics, Universität Hamburg, 22761 Hamburg, Germany*
[3] *Deutsches Elektronen-Synchrotron DESY, Notkestr. 85, 22607, Hamburg, Germany*
[4] *CENTRA, Departamento de Física, Instituto Superior Técnico – IST,*
Universidade de Lisboa – UL, Avenida Rovisco Pais 1, 1049 Lisboa, Portugal
(Dated: August 3, 2023)

Ultralight bosons can grow substantially in the vicinity of a black hole, through superradiant energy extraction. Consequently, such bosons can potentially reach field values close to the Planck scale, making black holes powerful transducers of such fields. If a scalar field couples to neutrino, it can trigger parametric production of neutrinos, and potentially quench their superradiant growth. During this saturation phase, scalar clouds can accelerate neutrinos to the TeV energy scale, generating fluxes that surpass those produced by atmospheric neutrinos.

Introduction. Hypothetical bosons with ultralight masses are promising candidates for beyond-the-standard-model particle physics. They are motivated by their potential to explain the smallness of the neutron electric dipole moment [1], and they are natural outcomes of fundamental theories with extra dimensions [2–5]. When these bosons comprise dark matter [6–9] and possess masses lower than $\mathcal{O}(1)\,\mathrm{eV}$, they behave as coherent waves due to their substantial occupation numbers [10].

The signals associated with ultralight bosons are typically proportional to their energy density or field value. When the Compton wavelength of these bosons is comparable to the gravitational radius of a rapidly rotating black hole (BH), a bound state can form through the superradiance mechanism, which involves the extraction of the BH rotational energy [11–13]. The process then leads to the condensation of a bosonic structure – a boson cloud – in the BH exterior [14–16]. Superradiant clouds can reach a total mass of approximately $\mathcal{O}(10)\%$ of the BH mass [17–19], corresponding to a field value approaching the Planck scale [20]. Thus, Kerr BHs can serve as powerful transducers for ultralight bosons [13]. Detection based on superradiance does not necessarily require ultralight bosons to constitute the majority of dark matter. It can be achieved, for example, through the spin-down of BHs [17, 21–30], gravitational-wave signals from boson clouds [20–24, 27, 31–44], and axion cloud-induced birefringence [45–48].

The couplings between ultralight bosons and standard model neutrinos are prevalent in various beyond-standard-model theories, which are motivated by neutrino mass generation [49–51] and grand unification theories [52–56]. Nevertheless, investigating these couplings presents significant challenges due to the inherent difficulties associated with neutrino production and detection. The constraints on these couplings primarily arise from neutrino self-interactions mediated by ultralight bosons [57–62], and distortions in neutrino oscillations caused by ultralight dark matter [63–82].

In this work, we demonstrate that scalar clouds surrounding BHs can generate substantial neutrino emissions through parametric production [83, 84]. Moreover, the spatial gradient of scalar clouds can efficiently accelerate the produced neutrinos to TeV-level energies. Given the significant field values achievable through superradiant production, a deeper range of coupling constants can be explored by comparing the anticipated fluxes with those observed in diffusive atmospheric neutrinos [85].

Superradiant Clouds. An ultralight boson field can form (quasi-)bound states outside a BH due to gravitational attraction. These bound states exhibit discrete quantum numbers and are influenced by the gravitational fine-structure constant, denoted as $\alpha \equiv G_{\mathrm{N}} M_{\mathrm{BH}} \mu$ [13, 14]. Here, G_{N} is Newton's constant, while M_{BH} and μ represent the BH mass and the boson mass, respectively. Superradiance occurs when the BH rotates at a sufficient velocity for its angular velocity to surpass the angular phase velocity of specific boson states, leading to exponential transfer of rotational energy into these states [12, 13].

We focus on the superradiant ground state of a massive scalar ϕ, whose orbital angular momentum corotates with the BH. Its wave function can be approximated as [14]

$$\phi(\vec{x}, t) = \Psi_0(t) R_\alpha(r) \sin\theta \cos(\mu t - \varphi), \quad (1)$$

in the Newtonian, $\alpha \ll 1$ limit. Here, Ψ_0 represents the peak field value of the scalar cloud, $R_\alpha(r) = \mathrm{Exp}[1 - \alpha^2 r/(2r_g)]\,\alpha^2 r/(2r_g)$ denotes the normalized radial potential. We adopt Boyer-Lindquist coordinates (t, r, θ, φ), and $r_g \equiv G_{\mathrm{N}} M_{\mathrm{BH}}$ represents the gravitational radius. It is worth noting that the total mass of the cloud, M_{cloud}, should not exceed approximately 10% of the BH mass. Beyond this threshold, the BH spin decreases to a value that no longer satisfies the superradiant condition, unless there is an external input of angular momentum to the BH. By considering the relationship

$M_{\text{cloud}} \approx 186\Psi_0^2/(\alpha^3\mu)$, we observe that the field value can approach the Planck scale:

$$\Psi_0 \approx 1.1 \times 10^{16}\,\text{GeV}\left(\frac{\alpha}{0.2}\right)^2\left(\frac{M_{\text{cloud}}}{0.1M_{\text{BH}}}\right)^{1/2}. \quad (2)$$

Hereafter, we adopt $\Psi_0^{10\%}$ as the maximum allowable field value by setting $M_{\text{cloud}}/M_{\text{BH}} = 0.1$ in Eq. (2).

On the other hand, exponential growth can be halted prior to the occurrence of a strong backreaction on the BH if there exists an interaction between the boson cloud and other fields. In such cases, the cloud reaches a quasi-equilibrium state where the interaction induces a steady outflow of energy, effectively balancing the superradiant gain. Examples of such interactions include quartic self-interactions [31, 86–88], axion-photon coupling [89–92], and electron-positron pair production [86, 93, 94].

Neutrino Emission from Scalar Clouds. We investigate a neutrino-philic coupling between a scalar field denoted as ϕ and the left-handed neutrino ν_L, which is described using two-component spinor notation:

$$g_{\phi\nu}\,\phi\,\nu_L\nu_L. \quad (3)$$

Here, $g_{\phi\nu}$ represents the coupling constant. The scalar field involved in this interaction is commonly referred to as the Majoron. Its coupling has been extensively discussed in the context of mediating neutrino self-interactions, a comprehensive summary can be found in Ref. [61]. Various constraints on the value of $g_{\phi\nu}$ exist when considering the case of an ultralight ϕ, including supernova (SN) 1987A [95, 96], double beta decay [59, 97], big bang nucleosynthesis [58], and the cosmic microwave background [60, 62]. These studies have established an approximate upper limit of $g_{\phi\nu} < 3 \times 10^{-7}$. For simplicity, we assume a universal coupling to all mass eigenstates in the following.

Given the significant field value that scalar clouds can attain and the light neutrino masses ($< 0.12\,\text{eV}$ [98, 99]), we expect that the coupling in Eq. (3) induces a coherent oscillating mass term $g_{\phi\nu}\phi$ for neutrinos around the cloud. The amplitude of this oscillation $g_{\phi\nu}\phi_0$ is more significant than the bare mass of neutrino m_ν, where $\phi_0 \equiv \Psi_0 R_\alpha(r)\sin\theta$ represents the local amplitude of the scalar field. When the effective mass, $m_{\text{eff}} = g_{\phi\nu}\phi + m_\nu$, crosses zero, neutrinos undergo parametric excitation. This production mechanism was previously studied during preheating [83, 84], and the average production rate per unit volume is given by

$$\Gamma_{\phi\nu} \approx \frac{g_{\phi\nu}^2\phi_0^2\mu^2}{48\pi^3}\sqrt{\frac{\mu}{g_{\phi\nu}\phi_0}}, \quad (4)$$

see Supplemental Material for details. Relativistic neutrinos are produced with an initial momentum $|\vec{p}_\nu^i| \sim$

$\sqrt{g_{\phi\nu}\phi_0\mu}/2$. The corresponding de Broglie wavelength of the neutrinos, $\sim 1/|\vec{p}_\nu^i|$, is significantly shorter than the size of the cloud, $\sim 1/(\alpha\mu)$. This allows us to safely ignore the finite-size effects when using Eq. (4).

Once produced, the neutrinos immediately experience an effective force arising from the varying mass term [100]. The equation of motion for their worldline is given by:

$$\frac{\mathrm{d}p_\nu^\alpha}{\mathrm{d}t} = -\frac{1}{p_\nu^0}\Gamma_{\kappa\beta}^\alpha\,p_\nu^\kappa\,p_\nu^\beta - \frac{1}{2p_\nu^0}\nabla^\alpha m_{\text{eff}}^2. \quad (5)$$

Here, p_ν^α represents the 4-momentum of the neutrinos, and $\Gamma_{\kappa\beta}^\alpha$ refers the Christoffel symbols of the Kerr metric. The spatial components of Eq. (5) contain the effective force $-\vec{\nabla}m_{\text{eff}}^2/(2p_\nu^0)$, which accelerates the neutrinos after their production. The final accelerated energy, denoted as ω_{acc}^ν, can be estimated by considering the 0-component of Eq. (5), resulting in $\omega_{\text{acc}}^\nu \sim g_{\phi\nu}\phi_0$. It is essential to emphasize that both the spatial gradient and temporal oscillation of the cloud wave-function are necessary for the acceleration process, as demonstrated in Eq. (5). Notably, neutrinos produced during the previous crossing, having been accelerated to much higher energies than $|\vec{p}_\nu^i|$, would not influence subsequent production, akin to the pair production of millicharged particles from superconducting cavities [101].

To obtain the angular distribution and spectrum of the outgoing neutrino fluxes, we perform simulations of neutrino trajectories originating from various points within scalar clouds. Details can be found in the Supplemental Material. The top panel of Fig. 1 presents two examples of neutrino trajectories emitted simultaneously from distances of $10\,r_g$ (shown in orange) and $100\,r_g$ (shown in green) in a scalar cloud background with $\alpha = 0.2$. Notably, the trajectory originating from the outer region directly leaves the cloud in the radial direction, while the other trajectory first curls around the BH spin axis (shown in black). Additionally, we depict the force lines from $-\vec{\nabla}\phi^2$ at the production time and density of ϕ_0^2 in gray. The bottom panel displays the outgoing spectrum as a function of the observer's inclination angle θ_o. The flux is slightly higher when observed from nearly face-on angles ($|\cos\theta_o| > 3/4$), forming a jet-like structure of neutrinos. This enhanced flux is primarily due to the tendency of neutrinos produced in the inner region of the cloud to be trapped in perpendicular directions while maintaining acceleration along the polar axis.

Based on our simulations, we have determined the average energy of the neutrino fluxes:

$$\bar{\omega}_{\text{acc}}^\nu \approx 2.7\,\text{TeV}\left(\frac{g_{\phi\nu}}{10^{-8}}\right)\left(\frac{\Psi_0}{10^{12}\,\text{GeV}}\right). \quad (6)$$

This value is generally independent of α, as demonstrated in the Supplemental Material. We can estimate the dif-
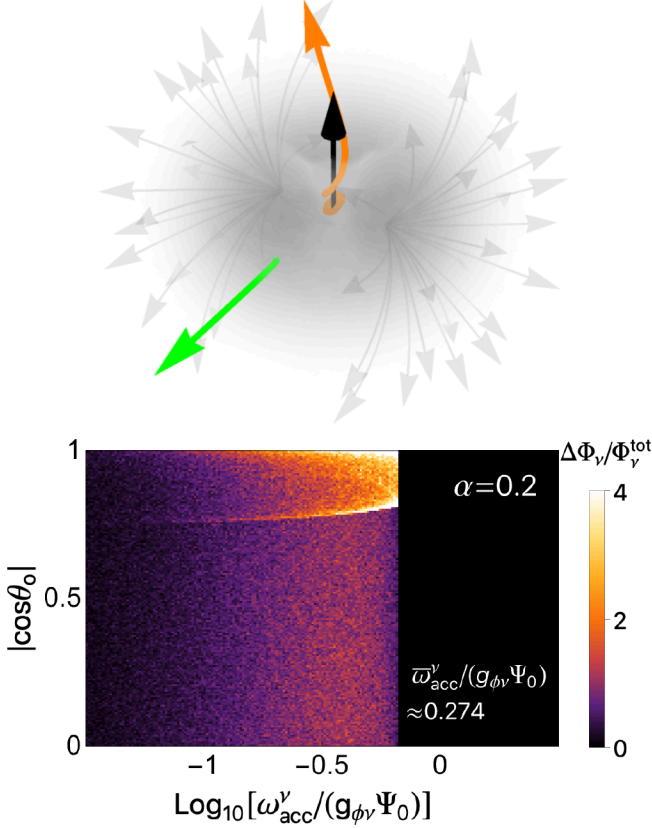
FIG. 1. Top panel: examples of neutrino trajectories originating simultaneously from distances of $10\,r_g$ (orange) and $100\,r_g$ (green) with respect to the BH. The direction of the black arrow indicates the BH spin. The scalar force lines present at the production time and the density of ϕ_0^2 are depicted in gray. Bottom panel: The observed neutrino energy spectrum $\Delta\Phi_\nu \equiv \mathrm{d}\Phi_\nu/(\mathrm{d}\cos\theta_o\,\mathrm{dlog}_{10}\omega_{\mathrm{acc}}^\nu)$ for distant observers located at inclination angles θ_o. Φ_ν^{tot} is the total flux emitted.

ferential fluxes received by a distant observer using

$$\frac{\mathrm{d}\Phi_\nu}{\mathrm{d}\omega_{\mathrm{acc}}^\nu}(\bar{\omega}_{\mathrm{acc}}^\nu) \approx \frac{3\int\Gamma_{\phi\nu}\,d^3\vec{x}}{4\pi d^2\,\bar{\omega}_{\mathrm{acc}}^\nu}$$

$$\simeq 1.2\times10^{-7}\,\mathrm{cm}^{-2}\mathrm{s}^{-1}\,\mathrm{GeV}^{-1}\left(\frac{g_{\phi\nu}}{10^{-8}}\right)^{1/2}\left(\frac{\Psi_0}{10^{12}\,\mathrm{GeV}}\right)^{1/2}$$

$$\times\left(\frac{10^{-12}\,\mathrm{eV}}{\mu}\right)^{1/2}\left(\frac{0.25}{\alpha}\right)^3\left(\frac{10\,\mathrm{kpc}}{d}\right)^2.$$

(7)

Here, the factor 3 accounts for the number of neutrino mass eigenstates, and d represents the distance between the BH and the observer.

We will now examine the value of Ψ_0 in the presence of neutrino production and acceleration. This condition can be solved by ensuring that the energy carried away by neutrinos balances the energy injected by the BH through superradiance, i.e.,

$$\Gamma_{\mathrm{SR}}^\phi\,M_{\mathrm{cloud}} = 3\,\bar{\omega}_{\mathrm{acc}}^\nu\int\Gamma_{\phi\nu}\,d^3\vec{x}.$$

(8)

Here, $\Gamma_{\mathrm{SR}}^\phi$ represents the scalar superradiant rate, which is approximately $\alpha^8 a_J\mu/24$ when $\alpha\ll 1$ [14]. The parameter a_J denotes the dimensionless spin parameter of the BH. Solving Eq. (8) yields the critical value for Ψ_0:

$$\Psi_0^c \approx 10^{12}\,\mathrm{GeV}\left(\frac{\mu}{10^{-12}\,\mathrm{eV}}\right)\left(\frac{\alpha}{0.25}\right)^{16}\left(\frac{10^{-8}}{g_{\phi\nu}}\right)^5\left(\frac{a_J}{0.9}\right)^2.$$

(9)

For the benchmark parameters, corresponding to a BH of mass $33\,M_\odot$, substituting the saturation field value from Eq. (9) into Eq. (6) and (7) yields steady emission of neutrinos with a typical energy scale of TeV and fluxes approximately equal to $1.2\times10^{-7}\,\mathrm{cm}^{-2}\mathrm{s}^{-1}\mathrm{GeV}^{-1}$. Notably, these values are significantly higher than the flux of atmospheric neutrinos, which is on the order of $10^{-11}\,\mathrm{cm}^{-2}\mathrm{s}^{-1}\mathrm{GeV}^{-1}$ at TeV [85]. Interestingly, both the neutrino fluxes and the average energy $\bar{\omega}_{\mathrm{acc}}^\nu$ during the saturation phase increase as $g_{\phi\nu}$ decreases. This behavior arises from the fact that a lower value of $g_{\phi\nu}$ leads to a higher critical amplitude Ψ_0^c.

Spin Measurements and Neutrino Detection. The key ingredients here are rapidly rotating BHs. Recent observations have confirmed the existence of both stellar-mass BHs and supermassive BHs, with masses ranging from a few $M_\odot$ to $10^{10}\,M_\odot$. Despite the lower scalar mass μ, which reduces the saturated neutrino fluxes and average energy, scalar clouds surrounding supermassive BHs can still generate and accelerate neutrinos, as long as $g_{\phi\nu}\Psi_0 \gg m_\nu$ [84]. Hence, we will consider both types of BHs in our analysis.

There are different methods for identifying stellar-mass BHs of interest, many of which rely on electromagnetic observations. One such method involves utilizing X-ray emissions to detect the motion of binary systems located at substantial distances [102]. Spectroscopic observations, such as iron lines, can provide further information about the spins of these BHs [103]. Another technique for identifying isolated BHs involves microlensing [104, 105]. Typically, these potential BH candidates are distributed throughout the Milky Way, with a distance of $\mathcal{O}(1)\,\mathrm{kpc}$ from Earth. Therefore, we adopt a benchmark value of $d = 1\,\mathrm{kpc}$ for stellar-mass BHs ranging from $3\,M_\odot$ to $100\,M_\odot$.

A different approach involves gravitational-wave observations [106]. When two BHs merge, they produce a BH remnant whose spin can be inferred from the gravitational wave signal. These events happen at distances typically exceeding $\mathcal{O}(10)\,\mathrm{Mpc}$. Nevertheless, for a critical field value Ψ_0^c close to $\Psi_0^{10\%}$, the neutrino fluxes continue to exceed the atmospheric background even at a distance of approximately Gpc. Consequently, we anticipate significant opportunities for neutrino detection following such merger events. Gravitational wave observations can serve as triggers for detecting neutrino signals,

which experience delayed arrival times due to superradiant timescales. The correlation between these two types of observations introduces novel prospects in the field of multi-messenger astronomy.

The remarkable advancements in Very-Long-Baseline Interferometry (VLBI) technology have enabled the observation of supermassive BHs. The Event Horizon Telescope, with unprecedented angular resolution, has captured horizon-scale images of two nearby supermassive BHs: M87* ($M_{\rm BH} \simeq 6.5 \times 10^9\,M_\odot$, $d \simeq 16.4\,{\rm Mpc}$) [107], and Sgr A* ($M_{\rm BH} \simeq 4.3 \times 10^6\,M_\odot$, $d \simeq 8.2\,{\rm kpc}$) [108]. These results are also in favor of nearly face-on observations and high spins of the two BHs. Moreover, there is promising potential to employ correlations between VLBI observations and neutrino experiments to investigate additional supermassive BHs located at greater distances [109]. An intriguing feature that can be anticipated from supermassive BHs is the periodic modulation of the neutrino flux. For instance, the cloud surrounding M87* oscillates with a period of $\mathcal{O}(10)\,{\rm days}$, a time span that is sufficiently long to be resolved.
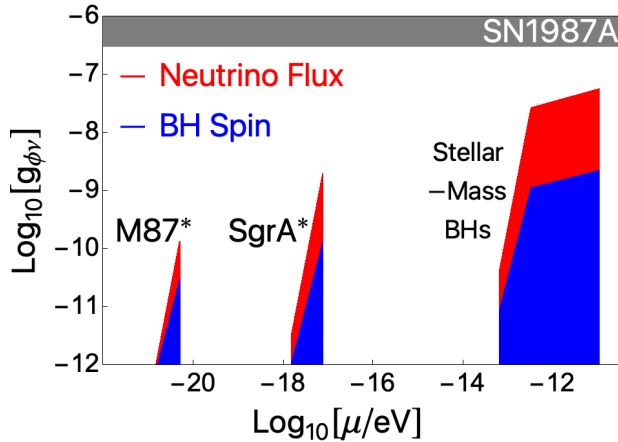

FIG. 2. Prospects for constraining the coupling $g_{\phi\nu}$ of a neutrino-philic scalar. The stellar-mass BHs considered have masses spanning from $3\,M_\odot$ to $100\,M_\odot$ and are assumed to be located at a distance of 1 kpc. The spin parameter is held constant at $a_J = 0.8$. Previous exclusion from SN1987A [95, 96] is shown for comparison.

When the interaction between ϕ and neutrinos is extremely weak, a steady state is not reached before the BH spins down. Consequently, detecting a BH with a high spin can rule out the corresponding superradiant window mass, similar to the constraints imposed on minimally coupled bosons or axions with weak self-interaction [17, 21–30]. A quantitative criterion for this exclusion is that $\Psi_0^c > \Psi_0^{10\%}$, which implies that the cloud extracts 10% of the BH energy without reaching the saturation phase. The blue region in Fig. 2 represents this condition. In our analysis, we consider a fixed spin parameter $a_J = 0.8$ with the highest possible value of $\alpha = 0.25$. The lower bound of α is set

at 0.05. For stellar-mass BHs, the corresponding scalar mass $\mu \equiv \alpha/(G_N M_{\rm BH})$, is divided into two regions. In the low-mass region, we fix $M_{\rm BH} = 100\,M_\odot$ and vary α from 0.05 to 0.25. In the high-mass region, we fix $\alpha = 0.25$ and vary $M_{\rm BH}$ from $100\,M_\odot$ to $3\,M_\odot$. We also include the constraints from the two nearby supermassive BHs.

The parameter space within the red region in Fig. 2 represents the range in which observable neutrino fluxes from a saturating cloud are expected. In this region, the cloud no longer exponentially extracts BH spin, thus enabling the coexistence of a high spin BH and the saturated cloud. Therefore, we maintain the value of $a_J = 0.8$, while μ follows the same division as the one used for spin measurement. The upper boundary of the blue region is determined by requiring the neutrino fluxes in Eq. (7) to be higher than 1% of the diffusive atmospheric neutrino background [85] at $\bar\omega_{\rm acc}^\nu$. The atmospheric neutrino has already been well measured by IceCube [110], Super-Kamiokande [111], ANTARES [112], and Baikal-GVD [113]. A target source with neutrino fluxes at 1% of the diffusive background can be easily distinguished with an angular resolution of $< 10°$ [114–119].

Discussion. Various intriguing phenomena can arise in the region of strong fields, particularly related to particle production. These phenomena have been previously examined in the preheating stage of the early universe [83, 84, 120, 121] and in the context of strong field quantum electrodynamics [122, 123]. Rotating BHs provide an excellent platform for studying particle production, as superradiant clouds can reach field values close to the Planck scale.

In this study, we propose a novel approach to investigate the interaction between ultralight bosonic fields and neutrinos through BH superradiance. Superradiant scalar clouds play dual roles in the generation and acceleration of neutrinos, necessitating both periodic oscillation and spatial gradient of the cloud wave-functions. The observation prospects can be examined from two perspectives. First, BH spin measurements can exclude negligible interactions with low values of $g_{\phi\nu}$. Second, neutrino fluxes from a target BH with high spin can constrain the region of strong interaction. Our findings demonstrate that the emitted neutrino fluxes can significantly surpass the diffusive background, both for stellar-mass BHs and supermassive BHs.

Apart from interactions involving a hidden scalar, it is also natural to consider interactions with a vector field in the presence of new gauge groups [52–56]. The vector cloud can generate neutrinos through Schwinger pair production [122, 123] and further accelerate them using the electric fields of the vector. However, the couplings between vector fields and neutrinos are subject

to strict constraints due to their coupling to other standard model fermions [124–130] or the non-conservation of currents [131–137]. Thus sophisticated model building is necessary in the neutrino sector to yield observable consequences.

Notice that the neutrino production from a bosonic cloud can also apply to other coupled fermions in the hidden sector. In addition, dark matter particles around the cloud can be directly accelerated to higher energies. Consequently the superradiant cloud can serve as a source for boosted dark matter, offering potential for detection through direct detection experiments and neutrino detectors [138–151]. The specific incoming directions of these particles can induce a daily modulation of signals due to scattering with Earth materials [152–157] or directional detectors [158].

---

* yifan.chen@nbi.ku.dk

† xiao.xue@desy.de

‡ vitor.cardoso@nbi.ku.dk

[1] R. D. Peccei and Helen R. Quinn, "CP Conservation in the Presence of Instantons," Phys. Rev. Lett. **38**, 1440–1443 (1977).

[2] Peter Svrcek and Edward Witten, "Axions In String Theory," JHEP **06**, 051 (2006), arXiv:hep-th/0605206.

[3] S. A. Abel, M. D. Goodsell, J. Jaeckel, V. V. Khoze, and A. Ringwald, "Kinetic Mixing of the Photon with Hidden U(1)s in String Phenomenology," JHEP **07**, 124 (2008), arXiv:0803.1449 [hep-ph].

[4] Asimina Arvanitaki, Savas Dimopoulos, Sergei Dubovsky, Nemanja Kaloper, and John March-Russell, "String Axiverse," Phys. Rev. **D81**, 123530 (2010), arXiv:0905.4720 [hep-th].

[5] Mark Goodsell, Joerg Jaeckel, Javier Redondo, and Andreas Ringwald, "Naturally Light Hidden Photons in LARGE Volume String Compactifications," JHEP **11**, 027 (2009), arXiv:0909.0515 [hep-ph].

[6] John Preskill, Mark B. Wise, and Frank Wilczek, "Cosmology of the Invisible Axion," Phys. Lett. **120B**, 127–132 (1983).

[7] L. F. Abbott and P. Sikivie, "A Cosmological Bound on the Invisible Axion," Phys. Lett. B **120**, 133–136 (1983).

[8] Michael Dine and Willy Fischler, "The Not So Harmless Axion," Phys. Lett. B **120**, 137–141 (1983).

[9] Ann E. Nelson and Jakub Scholtz, "Dark Light, Dark Matter and the Misalignment Mechanism," Phys. Rev. D **84**, 103501 (2011), arXiv:1105.2812 [hep-ph].

[10] Wayne Hu, Rennan Barkana, and Andrei Gruzinov, "Cold and fuzzy dark matter," Phys. Rev. Lett. **85**, 1158–1161 (2000), arXiv:astro-ph/0003365.

[11] R. Penrose and R. M. Floyd, "Extraction of rotational energy from a black hole," Nature **229**, 177–179 (1971).

[12] Ya. B. Zel'Dovich, "Generation of Waves by a Rotating Body," Soviet Journal of Experimental and Theoretical Physics Letters **14**, 180 (1971).

[13] Richard Brito, Vitor Cardoso, and Paolo Pani, "Superradiance: New Frontiers in Black Hole Physics," Lect. Notes Phys. **906**, pp.1–237 (2015), arXiv:1501.06570 [gr-qc].

[14] Steven L. Detweiler, "KLEIN-GORDON EQUATION AND ROTATING BLACK HOLES," Phys. Rev. D **22**, 2323–2326 (1980).

[15] Vitor Cardoso and Shijun Yoshida, "Superradiant instabilities of rotating black branes and strings," JHEP **07**, 009 (2005), arXiv:hep-th/0502206.

[16] Sam R. Dolan, "Instability of the massive Klein-Gordon field on the Kerr spacetime," Phys. Rev. D **76**, 084001 (2007), arXiv:0705.2880 [gr-qc].

[17] Richard Brito, Vitor Cardoso, and Paolo Pani, "Black holes as particle detectors: evolution of superradiant instabilities," Class. Quant. Grav. **32**, 134001 (2015), arXiv:1411.0686 [gr-qc].

[18] William E. East and Frans Pretorius, "Superradiant Instability and Backreaction of Massive Vector Fields around Kerr Black Holes," Phys. Rev. Lett. **119**, 041101 (2017), arXiv:1704.04791 [gr-qc].

[19] Carlos A. R. Herdeiro, Eugen Radu, and Nuno M. Santos, "A bound on energy extraction (and hairiness) from superradiance," Phys. Lett. B **824**, 136835 (2022), arXiv:2111.03667 [gr-qc].

[20] Yifan Chen, Xiao Xue, Richard Brito, and Vitor Cardoso, "Photon Ring Astrometry for Superradiant Clouds," Phys. Rev. Lett. **130**, 111401 (2023), arXiv:2211.03794 [gr-qc].

[21] Asimina Arvanitaki and Sergei Dubovsky, "Exploring the String Axiverse with Precision Black Hole Physics," Phys. Rev. **D83**, 044026 (2011), arXiv:1004.3558 [hep-th].

[22] Asimina Arvanitaki, Masha Baryakhtar, and Xinlu Huang, "Discovering the QCD Axion with Black Holes and Gravitational Waves," Phys. Rev. **D91**, 084011 (2015), arXiv:1411.2263 [hep-ph].

[23] Masha Baryakhtar, Robert Lasenby, and Mae Teo, "Black Hole Superradiance Signatures of Ultralight Vectors," Phys. Rev. D **96**, 035019 (2017), arXiv:1704.05081 [hep-ph].

[24] Richard Brito, Shrobana Ghosh, Enrico Barausse, Emanuele Berti, Vitor Cardoso, Irina Dvorkin, Antoine

Klein, and Paolo Pani, "Gravitational wave searches for ultralight bosons with LIGO and LISA," Phys. Rev. D **96**, 064050 (2017), arXiv:1706.06311 [gr-qc].

[25] Vitor Cardoso, Óscar J. C. Dias, Gavin S. Hartnett, Matthew Middleton, Paolo Pani, and Jorge E. Santos, "Constraining the mass of dark photons and axion-like particles through black-hole superradiance," JCAP **03**, 043 (2018), arXiv:1801.01420 [gr-qc].

[26] Hooman Davoudiasl and Peter B Denton, "Ultralight Boson Dark Matter and Event Horizon Telescope Observations of M87*," Phys. Rev. Lett. **123**, 021102 (2019), arXiv:1904.09242 [astro-ph.CO].

[27] Richard Brito, Sara Grillo, and Paolo Pani, "Black Hole Superradiant Instability from Ultralight Spin-2 Fields," Phys. Rev. Lett. **124**, 211101 (2020), arXiv:2002.04055 [gr-qc].

[28] Matthew J. Stott, "Ultralight Bosonic Field Mass Bounds from Astrophysical Black Hole Spin," (2020), arXiv:2009.07206 [hep-ph].

[29] Caner Ünal, Fabio Pacucci, and Abraham Loeb, "Properties of ultralight bosons from heavy quasar spins via superradiance," JCAP **05**, 007 (2021), arXiv:2012.12790 [hep-ph].

[30] Akash Kumar Saha, Priyank Parashari, Tarak Nath Maity, Abhishek Dubey, Subhadip Bouri, and Ranjan Laha, "Bounds on ultralight bosons from the Event Horizon Telescope observation of Sgr A*," (2022), arXiv:2208.03530 [astro-ph.HE].

[31] Hirotaka Yoshino and Hideo Kodama, "Bosenova collapse of axion cloud around a rotating black hole," Prog. Theor. Phys. **128**, 153–190 (2012), arXiv:1203.5070 [gr-qc].

[32] Hirotaka Yoshino and Hideo Kodama, "Gravitational radiation from an axion cloud around a black hole: Superradiant phase," PTEP **2014**, 043E02 (2014), arXiv:1312.2326 [gr-qc].

[33] Hirotaka Yoshino and Hideo Kodama, "The bosenova and axiverse," Class. Quant. Grav. **32**, 214001 (2015), arXiv:1505.00714 [gr-qc].

[34] Richard Brito, Shrobana Ghosh, Enrico Barausse, Emanuele Berti, Vitor Cardoso, Irina Dvorkin, Antoine Klein, and Paolo Pani, "Stochastic and resolvable gravitational waves from ultralight bosons," Phys. Rev. Lett. **119**, 131101 (2017), arXiv:1706.05097 [gr-qc].

[35] Maximiliano Isi, Ling Sun, Richard Brito, and Andrew Melatos, "Directed searches for gravitational waves from ultralight bosons," Phys. Rev. D **99**, 084042 (2019), [Erratum: Phys.Rev.D 102, 049901 (2020)], arXiv:1810.03812 [gr-qc].

[36] Nils Siemonsen and William E. East, "Gravitational wave signatures of ultralight vector bosons from black hole superradiance," Phys. Rev. D **101**, 024019 (2020), arXiv:1910.09476 [gr-qc].

[37] Ling Sun, Richard Brito, and Maximiliano Isi, "Search for ultralight bosons in Cygnus X-1 with Advanced LIGO," Phys. Rev. D **101**, 063020 (2020), [Erratum: Phys.Rev.D 102, 089902 (2020)], arXiv:1909.11267 [gr-qc].

[38] Cristiano Palomba et al., "Direct constraints on ultralight boson mass from searches for continuous gravitational waves," Phys. Rev. Lett. **123**, 171101 (2019), arXiv:1909.08854 [astro-ph.HE].

[39] Sylvia J. Zhu, Masha Baryakhtar, Maria Alessandra Papa, Daichi Tsuna, Norita Kawanaka, and Heinz-Bernd Eggenstein, "Characterizing the continuous gravitational-wave signal from boson clouds around Galactic isolated black holes," Phys. Rev. D **102**, 063020 (2020), arXiv:2003.03359 [gr-qc].

[40] Leo Tsukada, Richard Brito, William E. East, and Nils Siemonsen, "Modeling and searching for a stochastic gravitational-wave background from ultralight vector bosons," Phys. Rev. D **103**, 083005 (2021), arXiv:2011.06995 [astro-ph.HE].

[41] Chen Yuan, Richard Brito, and Vitor Cardoso, "Probing ultralight dark matter with future ground-based gravitational-wave detectors," Phys. Rev. D **104**, 044011 (2021), arXiv:2106.00021 [gr-qc].

[42] R. Abbott et al. (KAGRA, VIRGO, LIGO Scientific), "All-sky search for gravitational wave emission from scalar boson clouds around spinning black holes in LIGO O3 data," Phys. Rev. D **105**, 102001 (2022), arXiv:2111.15507 [astro-ph.HE].

[43] Chen Yuan, Yang Jiang, and Qing-Guo Huang, "Constraints on an ultralight scalar boson from Advanced LIGO and Advanced Virgo's first three observing runs using the stochastic gravitational-wave background," Phys. Rev. D **106**, 023020 (2022), arXiv:2204.03482 [astro-ph.CO].

[44] Richard Brito and Shreya Shah, "Extreme mass-ratio inspirals into black holes surrounded by scalar clouds," (2023), arXiv:2307.16093 [gr-qc].

[45] Yifan Chen, Jing Shu, Xiao Xue, Qiang Yuan, and Yue Zhao, "Probing Axions with Event Horizon Telescope Polarimetric Measurements," Phys. Rev. Lett. **124**, 061102 (2020), arXiv:1905.02213 [hep-ph].

[46] Guan-Wen Yuan, Zi-Qing Xia, Chengfeng Tang, Yaqi Zhao, Yi-Fu Cai, Yifan Chen, Jing Shu, and Qiang Yuan, "Testing the ALP-photon coupling with polarization measurements of Sagittarius A⋆," JCAP **03**, 018 (2021), arXiv:2008.13662 [astro-ph.HE].

[47] Yifan Chen, Yuxin Liu, Ru-Sen Lu, Yosuke Mizuno, Jing Shu, Xiao Xue, Qiang Yuan, and Yue Zhao, "Stringent axion constraints with Event Horizon Telescope polarimetric measurements of M87⋆," Nature Astron. **6**, 592–598 (2022), arXiv:2105.04572 [hep-ph].

[48] Yifan Chen, Chunlong Li, Yosuke Mizuno, Jing Shu, Xiao Xue, Qiang Yuan, Yue Zhao, and Zihan Zhou, "Birefringence tomography for axion cloud," JCAP **09**, 073 (2022), arXiv:2208.05724 [hep-ph].

[49] G. B. Gelmini and M. Roncadelli, "Left-Handed Neutrino Mass Scale and Spontaneously Broken Lepton Number," Phys. Lett. B **99**, 411–415 (1981).

[50] Y. Chikashige, Rabindra N. Mohapatra, and R. D. Peccei, "Are There Real Goldstone Bosons Associated with Broken Lepton Number?" Phys. Lett. B **98**, 265–268 (1981).

[51] C. S. Aulakh and Rabindra N. Mohapatra, "Neutrino as the Supersymmetric Partner of the Majoron," Phys. Lett. B **119**, 136–140 (1982).

[52] H. Georgi and S. L. Glashow, "Unity of All Elementary Particle Forces," Phys. Rev. Lett. **32**, 438–441 (1974).

[53] Jogesh C. Pati and Abdus Salam, "Lepton Number as the Fourth Color," Phys. Rev. D **10**, 275–289 (1974), [Erratum: Phys.Rev.D 11, 703–703 (1975)].

[54] Rabindra N. Mohapatra and Jogesh C. Pati, "Left-Right Gauge Symmetry and an Isoconjugate Model of CP Violation," Phys. Rev. D **11**, 566–571 (1975).

[55] Harald Fritzsch and Peter Minkowski, "Unified Interactions of Leptons and Hadrons," Annals Phys. **93**, 193–266 (1975).

[56] Howard Georgi, "The State of the Art—Gauge Theories," AIP Conf. Proc. **23**, 575–582 (1975).

[57] Edward W. Kolb and Michael S. Turner, "Supernova SN 1987a and the Secret Interactions of Neutrinos," Phys. Rev. D **36**, 2895 (1987).

[58] Guo-yuan Huang, Tommy Ohlsson, and Shun Zhou, "Observational Constraints on Secret Neutrino Interactions from Big Bang Nucleosynthesis," Phys. Rev. D **97**, 075009 (2018), arXiv:1712.04792 [hep-ph].

[59] Tim Brune and Heinrich Päs, "Massive Majorons and constraints on the Majoron-neutrino coupling," Phys. Rev. D **99**, 096005 (2019), arXiv:1808.08158 [hep-ph].

[60] Francesco Forastieri, Massimiliano Lattanzi, and Paolo Natoli, "Cosmological constraints on neutrino self-interactions with a light mediator," Phys. Rev. D **100**, 103526 (2019), arXiv:1904.07810 [astro-ph.CO].

[61] Jeffrey M. Berryman *et al.*, "Neutrino Self-Interactions: A White Paper," in *Snowmass 2021* (2022) arXiv:2203.01955 [hep-ph].

[62] Shao-Ping Li and Xun-Jie Xu, "N_{eff} constraints on light mediators coupled to neutrinos: the dilution-resistant effect," (2023), arXiv:2307.13967 [hep-ph].

[63] Matías M. Reynoso and Oscar A. Sampayo, "Propagation of high-energy neutrinos in a background of ultra-light scalar dark matter," Astropart. Phys. **82**, 10–20 (2016), arXiv:1605.09671 [hep-ph].

[64] Asher Berlin, "Neutrino Oscillations as a Probe of Light Scalar Dark Matter," Phys. Rev. Lett. **117**, 231801 (2016), arXiv:1608.01307 [hep-ph].

[65] Gordan Krnjaic, Pedro A. N. Machado, and Lina Necib, "Distorted neutrino oscillations from time varying cosmic fields," Phys. Rev. D **97**, 075017 (2018), arXiv:1705.06740 [hep-ph].

[66] Vedran Brdar, Joachim Kopp, Jia Liu, Pascal Prass, and Xiao-Ping Wang, "Fuzzy dark matter and nonstandard neutrino interactions," Phys. Rev. D **97**, 043001 (2018), arXiv:1705.09455 [hep-ph].

[67] Hooman Davoudiasl, Gopolang Mohlabeng, and Matthew Sullivan, "Galactic Dark Matter Population as the Source of Neutrino Masses," Phys. Rev. D **98**, 021301 (2018), arXiv:1803.00012 [hep-ph].

[68] Jiajun Liao, Danny Marfatia, and Kerry Whisnant, "Light scalar dark matter at neutrino oscillation experiments," JHEP **04**, 136 (2018), arXiv:1803.01773 [hep-ph].

[69] Francesco Capozzi, Ian M. Shoemaker, and Luca Vecchi, "Neutrino Oscillations in Dark Backgrounds," JCAP **07**, 004 (2018), arXiv:1804.05117 [hep-ph].

[70] Guo-Yuan Huang and Newton Nath, "Neutrinophilic Axion-Like Dark Matter," Eur. Phys. J. C **78**, 922 (2018), arXiv:1809.01111 [hep-ph].

[71] Yasaman Farzan, "Ultra-light scalar saving the 3 + 1 neutrino scheme from the cosmological bounds," Phys. Lett. B **797**, 134911 (2019), arXiv:1907.04271 [hep-ph].

[72] James M. Cline, "Viable secret neutrino interactions with ultralight dark matter," Phys. Lett. B **802**, 135182 (2020), arXiv:1908.02278 [hep-ph].

[73] Abhish Dev, Pedro A. N. Machado, and Pablo Martínez-Miravé, "Signatures of ultralight dark matter in neutrino oscillation experiments," JHEP **01**, 094 (2021), arXiv:2007.03590 [hep-ph].

[74] Marta Losada, Yosef Nir, Gilad Perez, and Yogev Shpilman, "Probing scalar dark matter oscillations with neutrino oscillations," JHEP **04**, 030 (2022), arXiv:2107.10865 [hep-ph].

[75] Guo-yuan Huang and Newton Nath, "Neutrino meets ultralight dark matter: $0\nu\beta\beta$ decay and cosmology," JCAP **05**, 034 (2022), arXiv:2111.08732 [hep-ph].

[76] Eung Jin Chun, "Neutrino Transition in Dark Matter," (2021), arXiv:2112.05057 [hep-ph].

[77] Abhish Dev, Gordan Krnjaic, Pedro Machado, and Harikrishnan Ramani, "Constraining feeble neutrino interactions with ultralight dark matter," Phys. Rev. D **107**, 035006 (2023), arXiv:2205.06821 [hep-ph].

[78] Marta Losada, Yosef Nir, Gilad Perez, Inbar Savoray, and Yogev Shpilman, "Parametric resonance in neutrino oscillations induced by ultra-light dark matter and implications for KamLAND and JUNO," JHEP **03**, 032 (2023), arXiv:2205.09769 [hep-ph].

[79] Dawid Brzeminski, Saurav Das, Anson Hook, and Clayton Ristow, "Constraining Vector Dark Matter with Neutrino experiments," (2022), arXiv:2212.05073 [hep-ph].

[80] Gonzalo Alonso-Álvarez, Katarina Bleau, and James M. Cline, "Distortion of neutrino oscillations by dark photon dark matter," Phys. Rev. D **107**, 055045 (2023), arXiv:2301.04152 [hep-ph].

[81] YeolLin ChoeJo, Yechan Kim, and Hye-Sung Lee, "Dirac-Majorana neutrino type conversion induced by an oscillating scalar dark matter," (2023), arXiv:2305.16900 [hep-ph].

[82] Marta Losada, Yosef Nir, Gilad Perez, Inbar Savoray, and Yogev Shpilman, "Time Dependent CP-even and CP-odd Signatures of Scalar Ultra-light Dark Matter in Neutrino Oscillations," (2023), arXiv:2302.00005 [hep-ph].

[83] Patrick B. Greene and Lev Kofman, "Preheating of fermions," Phys. Lett. B **448**, 6–12 (1999), arXiv:hep-ph/9807339.

[84] Patrick B. Greene and Lev Kofman, "On the theory of fermionic preheating," Phys. Rev. D **62**, 123516 (2000), arXiv:hep-ph/0003018.

[85] Edoardo Vitagliano, Irene Tamborra, and Georg Raffelt, "Grand Unified Neutrino Spectrum at Earth: Sources and Spectral Components," Rev. Mod. Phys. **92**, 45006 (2020), arXiv:1910.11878 [astro-ph.HE].

[86] Hajime Fukuda and Kazunori Nakayama, "Aspects of Nonlinear Effect on Black Hole Superradiance," JHEP **01**, 128 (2020), arXiv:1910.06308 [hep-ph].

[87] Masha Baryakhtar, Marios Galanis, Robert Lasenby, and Olivier Simon, "Black hole superradiance of self-interacting scalar fields," Phys. Rev. D **103**, 095019 (2021), arXiv:2011.11646 [hep-ph].

[88] Hidetoshi Omiya, Takuya Takahashi, Takahiro Tanaka, and Hirotaka Yoshino, "Impact of multiple modes on the evolution of self-interacting axion condensate around rotating black holes," (2022), arXiv:2211.01949 [gr-qc].

[89] João G. Rosa and Thomas W. Kephart, "Stimulated Axion Decay in Superradiant Clouds around Primordial Black Holes," Phys. Rev. Lett. **120**, 231102 (2018), arXiv:1709.06581 [gr-qc].

[90] Mateja Boskovic, Richard Brito, Vitor Cardoso, Taishi Ikeda, and Helvi Witek, "Axionic instabilities and new black hole solutions," Phys. Rev. D **99**, 035006 (2019),

arXiv:1811.04945 [gr-qc].

[91] Taishi Ikeda, Richard Brito, and Vitor Cardoso, "Blasts of Light from Axions," Phys. Rev. Lett. **122**, 081101 (2019), arXiv:1811.04950 [gr-qc].

[92] Thomas F. M. Spieksma, Enrico Cannizzaro, Taishi Ikeda, Vitor Cardoso, and Yifan Chen, "Superradiance: Axionic Couplings and Plasma Effects," (2023), arXiv:2306.16447 [gr-qc].

[93] Diego Blas and Samuel J. Witte, "Quenching Mechanisms of Photon Superradiance," Phys. Rev. D **102**, 123018 (2020), arXiv:2009.10075 [hep-ph].

[94] Nils Siemonsen, Cristina Mondino, Daniel Egana-Ugrinovic, Junwu Huang, Masha Baryakhtar, and William E. East, "Dark photon superradiance: Electrodynamics and multimessenger signals," Phys. Rev. D **107**, 075025 (2023), arXiv:2212.09772 [astro-ph.HE].

[95] M. Kachelriess, R. Tomas, and J. W. F. Valle, "Supernova bounds on Majoron emitting decays of light neutrinos," Phys. Rev. D **62**, 023004 (2000), arXiv:hep-ph/0001039.

[96] Yasaman Farzan, "Bounds on the coupling of the Majoron to light neutrinos from supernova cooling," Phys. Rev. D **67**, 073015 (2003), arXiv:hep-ph/0211375.

[97] A. Gando *et al.* (KamLAND-Zen), "Limits on Majoron-emitting double-beta decays of Xe-136 in the KamLAND-Zen experiment," Phys. Rev. C **86**, 021601 (2012), arXiv:1205.6372 [hep-ex].

[98] N. Aghanim *et al.* (Planck), "Planck 2018 results. VI. Cosmological parameters," Astron. Astrophys. **641**, A6 (2020), [Erratum: Astron.Astrophys. 652, C4 (2021)], arXiv:1807.06209 [astro-ph.CO].

[99] Jyotsna Singh and M. Ibrahim Mirza, "Challenges in Neutrino Mass Measurements," (2023), arXiv:2305.12654 [hep-ex].

[100] Jean-Philippe Uzan, Martin Pernot-Borràs, and Joel Bergé, "Effects of a scalar fifth force on the dynamics of a charged particle as a new experimental design to test chameleon theories," Phys. Rev. D **102**, 044059 (2020), arXiv:2006.03359 [gr-qc].

[101] Asher Berlin and Anson Hook, "Searching for Millicharged Particles with Superconducting Radio-Frequency Cavities," Phys. Rev. D **102**, 035010 (2020), arXiv:2001.02679 [hep-ph].

[102] Walter H. G. Lewin, Jan van Paradijs, and Edward Peter Jacobus van den Heuvel, *X-ray Binaries* (1997).

[103] Laura W. Brenneman and Christopher S. Reynolds, "Constraining Black Hole Spin Via X-ray Spectroscopy," Astrophys. J. **652**, 1028–1043 (2006), arXiv:astro-ph/0608502.

[104] Shude Mao, Martin C. Smith, P. Wozniak, A. Udalski, M. Szymanski M. Kubiak, G. Pietrzynski, I. Soszynski, and K. Zebrun, "Optical gravitational lensing experiment. ogle-1999-bul-32: the longest ever microlensing event - evidence for a stellar mass black hole?" Mon. Not. Roy. Astron. Soc. **329**, 349 (2002), arXiv:astro-ph/0108312.

[105] D. P. Bennett *et al.*, "Gravitational microlensing events due to stellar mass black holes," Astrophys. J. **579**, 639–659 (2002), arXiv:astro-ph/0109467.

[106] Leor Barack *et al.*, "Black holes, gravitational waves and fundamental physics: a roadmap," Class. Quant. Grav. **36**, 143001 (2019), arXiv:1806.05195 [gr-qc].

[107] Kazunori Akiyama *et al.* (Event Horizon Telescope), "First M87 Event Horizon Telescope Results. I. The Shadow of the Supermassive Black Hole," Astrophys. J. Lett. **875**, L1 (2019), arXiv:1906.11238 [astro-ph.GA].

[108] Kazunori Akiyama *et al.* (Event Horizon Telescope), "First Sagittarius A* Event Horizon Telescope Results. I. The Shadow of the Supermassive Black Hole in the Center of the Milky Way," Astrophys. J. Lett. **930**, L12 (2022).

[109] Y. Y. Kovalev, A. V. Plavin, A. B. Pushkarev, and S. V. Troitsky, "Probing neutrino production in blazars by millimeter VLBI," Galaxies **11**, 84 (2023), arXiv:2307.02267 [astro-ph.HE].

[110] M. G. Aartsen *et al.* (IceCube), "Measurement of the Atmospheric ν_e Spectrum with IceCube," Phys. Rev. D **91**, 122004 (2015), arXiv:1504.03753 [astro-ph.HE].

[111] E. Richard *et al.* (Super-Kamiokande), "Measurements of the atmospheric neutrino flux by Super-Kamiokande: energy spectra, geomagnetic effects, and solar modulation," Phys. Rev. D **94**, 052001 (2016), arXiv:1510.08127 [hep-ex].

[112] A. Albert *et al.* (ANTARES), "All-flavor Search for a Diffuse Flux of Cosmic Neutrinos with Nine Years of ANTARES Data," Astrophys. J. Lett. **853**, L7 (2018), arXiv:1711.07212 [astro-ph.HE].

[113] V. A. Allakhverdyan *et al.* (Baikal-GVD), "Diffuse neutrino flux measurements with the Baikal-GVD neutrino telescope," Phys. Rev. D **107**, 042005 (2023), arXiv:2211.09447 [astro-ph.HE].

[114] M. G. Aartsen *et al.* (IceCube), "Energy Reconstruction Methods in the IceCube Neutrino Telescope," JINST **9**, P03009 (2014), arXiv:1311.4767 [physics.ins-det].

[115] S. Aiello *et al.* (KM3NeT), "Sensitivity of the KM3NeT/ARCA neutrino telescope to point-like neutrino sources," Astropart. Phys. **111**, 100–110 (2019), arXiv:1810.08499 [astro-ph.HE].

[116] M. G. Aartsen *et al.* (IceCube), "Search for steady point-like sources in the astrophysical muon neutrino flux with 8 years of IceCube data," Eur. Phys. J. C **79**, 234 (2019), arXiv:1811.07979 [hep-ph].

[117] M. G. Aartsen *et al.* (IceCube-Gen2), "IceCube-Gen2: the window to the extreme Universe," J. Phys. G **48**, 060501 (2021), arXiv:2008.04323 [astro-ph.HE].

[118] Damiano F. G. Fiorillo, Mauricio Bustamante, and Victor B. Valera, "Near-future discovery of point sources of ultra-high-energy neutrinos," JCAP **03**, 026 (2023), arXiv:2205.15985 [astro-ph.HE].

[119] R. Abbasi *et al.* (IceCube), "Observation of high-energy neutrinos from the Galactic plane," Science **380**, 6652 (2023), arXiv:2307.04427 [astro-ph.HE].

[120] Ya. B. Zeldovich and Alexei A. Starobinsky, "Particle production and vacuum polarization in an anisotropic gravitational field," Zh. Eksp. Teor. Fiz. **61**, 2161–2175 (1971).

[121] Lev Kofman, Andrei D. Linde, and Alexei A. Starobinsky, "Towards the theory of reheating after inflation," Phys. Rev. D **56**, 3258–3295 (1997), arXiv:hep-ph/9704452.

[122] Julian S. Schwinger, "On gauge invariance and vacuum polarization," Phys. Rev. **82**, 664–679 (1951).

[123] A.A. Grib, S.G. Mamayev, V.M. Mostepanenko, and V.M. Mostepanenko, *Vacuum Quantum Effects in Strong Fields* (Friedmann Laboratory Pub., 1994).

[124] Peter W. Graham, David E. Kaplan, Jeremy Mardon, Surjeet Rajendran, and William A. Terrano, "Dark Matter Direct Detection with Accelerometers," Phys.

Rev. D **93**, 075029 (2016), arXiv:1512.06165 [hep-ph].

[125] Aaron Pierce, Keith Riles, and Yue Zhao, "Searching for Dark Photon Dark Matter with Gravitational Wave Detectors," Phys. Rev. Lett. **121**, 061102 (2018), arXiv:1801.10161 [hep-ph].

[126] R. Abbott *et al.* (LIGO Scientific, KAGRA, Virgo), "Constraints on dark photon dark matter using data from LIGO's and Virgo's third observing run," Phys. Rev. D **105**, 063030 (2022), arXiv:2105.13085 [astro-ph.CO].

[127] E. A. Shaw, M. P. Ross, C. A. Hagedorn, E. G. Adelberger, and J. H. Gundlach, "Torsion-balance search for ultralow-mass bosonic dark matter," Phys. Rev. D **105**, 042007 (2022), arXiv:2109.08822 [astro-ph.CO].

[128] Xiao Xue *et al.* (PPTA), "High-precision search for dark photon dark matter with the Parkes Pulsar Timing Array," Phys. Rev. Res. **4**, L012022 (2022), arXiv:2112.07687 [hep-ph].

[129] Shao-Feng Ge and Pedro Pasquini, "Probing light mediators in the radiative emission of neutrino pair," Eur. Phys. J. C **82**, 208 (2022), arXiv:2110.03510 [hep-ph].

[130] Jiang-Chuan Yu, Yue-Hui Yao, Yong Tang, and Yue-Liang Wu, "Sensitivity of Space-based Gravitational-Wave Interferometers to Ultralight Bosonic Fields and Dark Matter," (2023), arXiv:2307.09197 [gr-qc].

[131] Ranjan Laha, Basudeb Dasgupta, and John F. Beacom, "Constraints on New Neutrino Interactions via Light Abelian Vector Bosons," Phys. Rev. D **89**, 093025 (2014), arXiv:1304.3460 [hep-ph].

[132] Pouya Bakhti and Yasaman Farzan, "Constraining secret gauge interactions of neutrinos by meson decays," Phys. Rev. D **95**, 095008 (2017), arXiv:1702.04187 [hep-ph].

[133] Miguel Escudero, Dan Hooper, Gordan Krnjaic, and Mathias Pierre, "Cosmology with A Very Light $L_\mu - L_\tau$ Gauge Boson," JHEP **03**, 071 (2019), arXiv:1901.02010 [hep-ph].

[134] Majid Bahraminasr, Pouya Bakhti, and Meshkat Rajaee, "Sensitivities to secret neutrino interaction at FASERν," J. Phys. G **48**, 095001 (2021), arXiv:2003.09985 [hep-ph].

[135] Jeff A. Dror, "Discovering leptonic forces using nonconserved currents," Phys. Rev. D **101**, 095013 (2020), arXiv:2004.04750 [hep-ph].

[136] Majid Ekhterachian, Anson Hook, Soubhik Kumar, and Yuhsin Tsai, "Bounds on gauge bosons coupled to nonconserved currents," Phys. Rev. D **104**, 035034 (2021), arXiv:2103.13396 [hep-ph].

[137] Masoom Singh, Mauricio Bustamante, and Sanjib Kumar Agarwalla, "Flavor-dependent long-range neutrino interactions in DUNE & T2HK: alone they constrain, together they discover," (2023), arXiv:2305.05184 [hep-ph].

[138] Francesco D'Eramo and Jesse Thaler, "Semi-annihilation of Dark Matter," JHEP **06**, 109 (2010), arXiv:1003.5912 [hep-ph].

[139] Junwu Huang and Yue Zhao, "Dark Matter Induced Nucleon Decay: Model and Signatures," JHEP **02**, 077 (2014), arXiv:1312.0011 [hep-ph].

[140] Kaustubh Agashe, Yanou Cui, Lina Necib, and Jesse Thaler, "(In)direct Detection of Boosted Dark Matter," JCAP **10**, 062 (2014), arXiv:1405.7370 [hep-ph].

[141] Joachim Kopp, Jia Liu, and Xiao-Ping Wang, "Boosted Dark Matter in IceCube and at the Galactic Center,"

JHEP **04**, 105 (2015), arXiv:1503.02669 [hep-ph].

[142] Atri Bhattacharya, Raj Gandhi, Aritra Gupta, and Satyanarayan Mukhopadhyay, "Boosted Dark Matter and its implications for the features in IceCube HESE data," JCAP **05**, 002 (2017), arXiv:1612.02834 [hep-ph].

[143] Ayuki Kamada, Hee Jung Kim, Hyungjin Kim, and Toyokazu Sekiguchi, "Self-Heating Dark Matter via Semiannihilation," Phys. Rev. Lett. **120**, 131802 (2018), arXiv:1707.09238 [hep-ph].

[144] C. Kachulis *et al.* (Super-Kamiokande), "Search for Boosted Dark Matter Interacting With Electrons in Super-Kamiokande," Phys. Rev. Lett. **120**, 221301 (2018), arXiv:1711.05278 [hep-ex].

[145] Animesh Chatterjee, Albert De Roeck, Doojin Kim, Zahra Gh. Moghaddam, Jong-Chul Park, Seodong Shin, Leigh H. Whitehead, and Jaehoon Yu, "Searching for boosted dark matter at ProtoDUNE," Phys. Rev. D **98**, 075027 (2018), arXiv:1803.03264 [hep-ph].

[146] Ayuki Kamada, Hee Jung Kim, and Hyungjin Kim, "Self-heating of Strongly Interacting Massive Particles," Phys. Rev. D **98**, 023509 (2018), arXiv:1805.05648 [hep-ph].

[147] David McKeen and Nirmal Raj, "Monochromatic dark neutrinos and boosted dark matter in noble liquid direct detection," Phys. Rev. D **99**, 103003 (2019), arXiv:1812.05102 [hep-ph].

[148] C. A. Argüelles *et al.*, "New opportunities at the next-generation neutrino experiments I: BSM neutrino physics and dark matter," Rept. Prog. Phys. **83**, 124201 (2020), arXiv:1907.08311 [hep-ph].

[149] Ayuki Kamada and Hee Jung Kim, "Escalating core formation with dark matter self-heating," Phys. Rev. D **102**, 043009 (2020), arXiv:1911.09717 [hep-ph].

[150] Joshua Berger, Yanou Cui, Mathew Graham, Lina Necib, Gianluca Petrillo, Dane Stocks, Yun-Tse Tsai, and Yue Zhao, "Prospects for detecting boosted dark matter in DUNE through hadronic interactions," Phys. Rev. D **103**, 095012 (2021), arXiv:1912.05558 [hep-ph].

[151] Babak Abi *et al.* (DUNE), "Deep Underground Neutrino Experiment (DUNE), Far Detector Technical Design Report, Volume II: DUNE Physics," (2020), arXiv:2002.03005 [hep-ex].

[152] Shao-Feng Ge, Jianglai Liu, Qiang Yuan, and Ning Zhou, "Diurnal Effect of Sub-GeV Dark Matter Boosted by Cosmic Rays," Phys. Rev. Lett. **126**, 091804 (2021), arXiv:2005.09480 [hep-ph].

[153] Bartosz Fornal, Pearl Sandick, Jing Shu, Meng Su, and Yue Zhao, "Boosted Dark Matter Interpretation of the XENON1T Excess," Phys. Rev. Lett. **125**, 161804 (2020), arXiv:2006.11264 [hep-ph].

[154] Yifan Chen, Bartosz Fornal, Pearl Sandick, Jing Shu, Xiao Xue, Yue Zhao, and Junchao Zong, "Earth shielding and daily modulation from electrophilic boosted dark particles," Phys. Rev. D **107**, 033006 (2023), arXiv:2110.09685 [hep-ph].

[155] Chen Xia, Yan-Hao Xu, and Yu-Feng Zhou, "Production and attenuation of cosmic-ray boosted dark matter," JCAP **02**, 028 (2022), arXiv:2111.05559 [hep-ph].

[156] Xiangyi Cui *et al.* (PandaX-II), "Search for Cosmic-Ray Boosted Sub-GeV Dark Matter at the PandaX-II Experiment," Phys. Rev. Lett. **128**, 171801 (2022), arXiv:2112.08957 [hep-ex].

[157] Mai Qiao, Chen Xia, and Yu-Feng Zhou, "Diurnal modulation of electron recoils from DM-nucleon scattering

through the Migdal effect," (2023), arXiv:2307.12820 [hep-ph].

[158] Sven E. Vahsen, Ciaran A. J. O'Hare, and Dinesh Loomba, "Directional Recoil Detection," Ann. Rev. Nucl. Part. Sci. **71**, 189–224 (2021), arXiv:2102.04596 [physics.ins-det].

[159] George Casella, Christian Robert, and Martin Wells, "Generalized accept-reject sampling schemes," Lecture Notes-Monograph Series **45** (2004), 10.1214/lnms/1196285403.

Supplemental Material: Black Holes as Neutrino Factories

Particle Production from Time-Varying Backgrounds

We begin by considering a bosonic field χ in a time-varying background [120, 121]. The equation of motion in the frequency domain can be expressed as

$$\ddot{\chi}_k + \omega_k(t)^2 \chi_k = 0. \tag{S1}$$

Here, $\omega_k(t)$ represents the time-varying energy, which is modulated by the background fields to which χ couples. The solutions to Eq. (S1) in the adiabatic representation are given by [121]

$$\chi_k(t) = \frac{\alpha_k(t)}{\sqrt{2\omega_k}} e^{-i \int_0^t \omega_k dt} + \frac{\beta_k(t)}{\sqrt{2\omega_k}} e^{+i \int_0^t \omega_k dt}. \tag{S2}$$

The coefficients α_k and β_k satisfy the following equations:

$$\dot{\alpha}_k = \frac{\dot{\omega}_k}{2\omega_k} e^{+2i \int_0^t \omega_k dt} \beta_k, \quad \dot{\beta}_k = \frac{\dot{\omega}_k}{2\omega_k} e^{-2i \int_0^t \omega_k dt} \alpha_k, \tag{S3}$$

and they adhere to the normalization condition $|\alpha_k|^2 - |\beta_k|^2 = 1$. Initially, at $t = 0$, the vacuum state is defined as $\alpha_k = 1$ and $\beta_k = 0$. The quantities $\alpha_k(t)$ and $\beta_k(t)$ correspond to the coefficients of the Bogoliubov transformation of the creation and annihilation operators, respectively, which diagonalize the Hamiltonian at each moment in time t. The particle occupation number for a momentum mode k is given by $n_k = |\beta_k|^2$, which yields the particle number density per unit volume as

$$n_\chi = \frac{1}{2\pi^2} \int_0^\infty dk k^2 |\beta_k|^2. \tag{S4}$$

When $|\beta_k| \ll 1$ holds true, we can approximate the solution for Eq. (S3) as

$$\beta_k \simeq \int_0^t dt' \frac{\dot{\omega}}{2\omega} \exp\left(-2i \int_0^{t'} dt'' \omega(t'')\right). \tag{S5}$$

Consequently, efficient particle production is expected when the non-adiabatic condition is satisfied:

$$\left|\frac{\dot{\omega}}{\omega^2}\right| \gg 1. \tag{S6}$$

Using the interaction term $g_{\phi\chi}^2 \phi^2 \chi^2 / 2$ as an example, we consider the following scenario: $\phi = \phi_0 \cos(\mu t)$ represents the coherently oscillating background scalar with amplitude ϕ_0 and frequency μ, and $g_{\phi\chi}$ represents the coupling constant. The frequency relation for χ is [121]

$$\omega_\chi^2 = k^2 + m_\chi^2 + g_{\phi\chi}^2 \phi_0^2 \cos^2(\mu t). \tag{S7}$$

Here, m_χ denotes the bare mass term of χ. In this context, our focus lies on the region where $g_{\phi\chi}^2 \phi_0^2 / \mu^2$ is substantially greater than 1, while m_χ can be considered negligible. Within a narrow region of ϕ during a single oscillation period, momentum values below the typical scale $k_\star = \sqrt{g_{\phi\chi} \phi_0 \mu}/2$ satisfy the non-adiabatic condition (S6). Consequently, the occupation number n_k for $k < k_\star$ is exponentially produced with a time dependence of approximately $\exp(2\mu\tau_k t)$, where $\tau_k \approx \mathcal{O}(0.1)$ [121].

Fermionic fields with a Yukawa coupling $g_{\phi\nu} \phi \nu_L \nu_L$ and a bare mass m_ν exhibit a frequency relation for the mode function given by [83, 84]

$$\omega_\nu^2 = k^2 + (m_\nu + g_{\phi\nu} \phi_0 \cos(\mu t))^2. \tag{S8}$$

In the near black hole region where the resonance parameter $q \equiv g_{\phi\nu}^2 \phi_0^2 / \mu^2$ is significantly high and $g_{\phi\nu} \phi_0 \gg m_\nu$, the non-adiabatic condition is met when the effective mass term, $m_{\text{eff}} \equiv m_\nu + g_{\phi\nu} \phi_0 \cos(\mu t)$, crosses zero. During each crossing, the background ground instantly contributes to the k−mode with a factor of $|\beta_k|^2 = e^{-\pi k^2/(g_{\phi\nu} \phi_0 \mu)} +$

$\cdots$ [83, 84], where $\cdots$ contains the terms related to previously produced fermions. Exponential growth is excluded due to Pauli blocking. Instead, a fermion sphere with a radius of approximately $k_\star = \sqrt{g_{\phi\nu}\phi_0\mu}/2$ is formed immediately after a single kick. In cases where neutrinos are produced from a superradiant scalar background, neutrinos produced during the previous kick are accelerated to much higher energy scales and will not obstruct subsequent production. Consequently, the average production rate per unit volume is estimated as:

$$\Gamma_{\phi\nu} \approx \frac{1}{2\pi^2}\frac{k_\star^3}{3}\frac{\mu}{\pi} = \frac{g_{\phi\nu}^2\phi_0^2\mu^2}{48\pi^3}\sqrt{\frac{\mu}{g_{\phi\nu}\phi_0}}. \tag{S9}$$

Here, the factor π/μ accounts for the time between two crossings. Furthermore, the de Broglie wavelength of the initially produced fermions, approximately $2\pi/k_\star$, is considerably shorter than the cloud size. Thus, the finite size of the cloud can be disregarded when considering the production rate.

The scalar cloud displays an oscillatory component in its wavefunction, which exhibits a dependency on the azimuthal angle, i.e., $\phi \propto \cos(\mu t - \varphi)$. This dependence arises from the orbital angular momentum of the cloud. Notably, at a specific time t, the non-adiabatic condition is triggered on a plane that is approximately aligned with $\varphi = \mu t \pm \pi/2$. As a result, the cloud oscillation induces a periodic rotation of the production plane around the spin axis of the black hole.

One key difference between boson and fermion production is the requirement for the bare mass term. In Eq. (S8), the effective mass is the linear sum of the bare mass and the oscillating term, so only $g_{\phi\nu}\phi_0 \gg m_\nu$ is necessary to trigger the parametric excitation [84]. On the other hand, for bosons, m_χ needs to be smaller than $k_\star$ due to their similar roles in Eq. (S8). In our cases, due to the smallness of the neutrino mass and the significant field value of the scalar cloud, neutrino production can be achieved for both stellar-mass black holes and supermassive black holes with different ranges of μ.

Neutrino Trajectory

Immediately after production, neutrinos start propagating under the scalar background outside the black hole. This is effectively equivalent to considering geodesics with a varying mass term denoted by $m_{\text{eff}} = g_{\phi\nu}\phi + m_\nu$. The worldline action for the neutrino is given by:

$$S_\nu = -\int d\tau\, m_{\text{eff}}\sqrt{-g_{\alpha\beta}u_\nu^\alpha u_\nu^\beta}, \tag{S10}$$

where $g_{\alpha\beta}$ is the Kerr metric, and u_ν^α is the 4-velocity of the neutrino particle. From Eq. (S10), we obtain the corresponding Euler-Lagrange equation:

$$\frac{du_\nu^\alpha}{d\tau} = -\Gamma_{\kappa\beta}^\alpha u_\nu^\kappa u_\nu^\beta - (g^{\alpha\beta} + u_\nu^\alpha u_\nu^\beta)\frac{\nabla_\beta m_{\text{eff}}}{m_{\text{eff}}}, \tag{S11}$$

where τ is the proper time, and $\Gamma_{\kappa\beta}^\alpha$ are the Christoffel symbols of the Kerr metric. By using the relations $p_\nu^\alpha = m_{\text{eff}}u_\nu^\alpha$ and $dt = u_\nu^0 d\tau$, we can rewrite Eq. (S11) as:

$$\frac{dp_\nu^\alpha}{dt} = -\frac{1}{p_\nu^0}\Gamma_{\kappa\beta}^\alpha p_\nu^\kappa p_\nu^\beta - \frac{1}{2p_\nu^0}\nabla^\alpha m_{\text{eff}}^2. \tag{S12}$$

Here, p_ν^0 satisfies the on-shell condition $p_\nu^0 = \sqrt{m_{\text{eff}}^2 + |\vec{p}_\nu|^2}$. The time-component of Eq. (S12) shows that p_ν^0 will be accelerated to the same order as m_{eff} after a time-scale of approximately $1/\mu$.

The two terms on the right-hand side of Eq. (S12) correspond to gravitational lensing and scalar force [100], respectively. We compare their relative contributions using Cartesian coordinates (t, x, y, z):

$$-\frac{\Gamma_{\kappa\beta}^\alpha p_\nu^\kappa p_\nu^\beta}{m_{\text{eff}}^2/r_g} \approx -\frac{r_g^2}{r^2}\left(\mathcal{O}(1) + \mathcal{O}(\frac{r_g}{r})\right), \tag{S13}$$

$$-\frac{\vec{\nabla}m_{\text{eff}}^2}{m_{\text{eff}}^2/r_g} = \alpha^2\,\hat{r} - \frac{2\,r_g}{r\cos(\alpha t - \phi)\sin\theta}\hat{n}_\perp + \cdots. \tag{S14}$$

Here, $\cdots$ represents the influence of the neutrino bare term m_ν, which is negligible in the region where $g_{\phi\nu}\phi_0 \gg m_\nu$. $\hat{n}_\perp \equiv (\cos(\alpha t), \sin(\alpha t), 0)$ is a unit directional vector rotating on the $x - y$ plane. It is clear that the scalar force

dominates over gravitational lensing in the majority part of the cloud. Thus, in the simulation, we neglect the effect of the latter.

When neutrinos are produced at larger radii, the first term on the right-hand side of Eq. (S14) dominates, accelerating neutrinos along the radial direction. This causes the nearly isotropic distribution of fluxes in Fig. 1 of the main text for $|\cos\theta_o| < 3/4$. On the other hand, the second term on the right-hand side of Eq. (S14) is non-negligible in the inner region of the cloud. It traps the trajectories in regions with small inclination angles ($|\cos\theta_o| > 3/4$), causing an excess of neutrino flux.

Trajectory and Flux Simulation

In this section, we will discuss the simulation of neutrino trajectories and the recording of the flux at infinity. For convenience, we introduce dimensionless quantities:

$$(\tilde{t}, \tilde{x}, \tilde{y}, \tilde{z}) \equiv (t/r_g, x/r_g, y/r_g, z/r_g), \qquad \tilde{p}_\nu^\alpha \equiv \frac{p_\nu^\alpha}{g_{\phi\nu}\Psi_0}, \quad \tilde{m}_{\rm eff} \equiv \frac{m_{\rm eff}}{g_{\phi\nu}\Psi_0}. \tag{S15}$$

The trajectories with these new definitions become:

$$\frac{d\tilde{x}^\alpha}{d\tilde{t}} = \frac{\tilde{p}_\nu^\alpha}{\tilde{p}_\nu^0}, \qquad \frac{d\tilde{p}_\nu^\alpha}{d\tilde{t}} = -\frac{\nabla^\alpha \tilde{m}_{\rm eff}^2}{2\tilde{p}_\nu^0}, \qquad \tilde{p}_\nu^0 = \sqrt{\tilde{m}_{\rm eff}^2 + |\vec{\tilde{p}}_\nu|^2}. \tag{S16}$$

We employ a Monte-Carlo simulation to generate neutrino events, where the initial positions of events are distributed within $2 < r/r_g < 40/\alpha^2$. The upper range is chosen to be much higher than the cloud size. We use the generalized acceptance-rejection method [159] for the distribution weighted by the production rate $\Gamma_{\phi\nu} \propto \phi_0^{3/2}$. Without loss of generality, we set the initial time of each event at $\tilde{t} = 0$. We relocate the azimuthal angle φ to either $\pi/2$ or $-\pi/2$, depending on the initial sign of φ.

To solve the trajectory of each event using Eq. (S16), we need to specify the initial momentum and the neutrino bare mass. The oscillatory part of the mass takes a value to cancel the bare mass, resulting in a vanishing $\tilde{m}_{\rm eff}$. Both the initial momentum with a value below $\tilde{k}_\star = \sqrt{\phi_0\mu/(g_{\phi\nu}\Psi_0^2)}/2$ and the dimensionless neutrino mass $m_\nu/(g_{\phi\nu}\Psi_0)$ are several orders of magnitude lower than 1 in the relevant parameter space of this work. We test the convergence of the trajectories, which demonstrates independence of the initial momentum value and directions. This is because the scalar background immediately contributes to $\mathcal{O}(1)$ values for both $\tilde{m}_{\rm eff}$ and $|\vec{\tilde{p}}_\nu|$. Hence, in practice, we choose a small enough value of momentum with random directions and vanishing $\tilde{m}_{\rm eff}$ as the initial condition.

The end of each trajectory is set to be at $\tilde{t} = 400/\alpha^2$, where both the momentum and outgoing direction (θ, φ) converge to nearly constant values. We assume that the observation takes a time longer than the oscillation period $2\pi/\mu$, allowing us to neglect the azimuthal angle φ dependence of the event. The final momentum and polar angle information are then recorded as

$$\omega_{\rm acc}^\nu/(g_{\phi\nu}\Psi_0) = \tilde{p}_\nu^0, \qquad \cos\theta_o = \tilde{p}_\nu^z/\tilde{p}_\nu^0, \tag{S17}$$

respectively. In Fig. 1 of the main text, we show the results for $\alpha = 0.2$, while in Fig. S1, we present the results for $\alpha = 0.05$ and 0.4 for comparison. The average momentum turns out to be universal for different α.
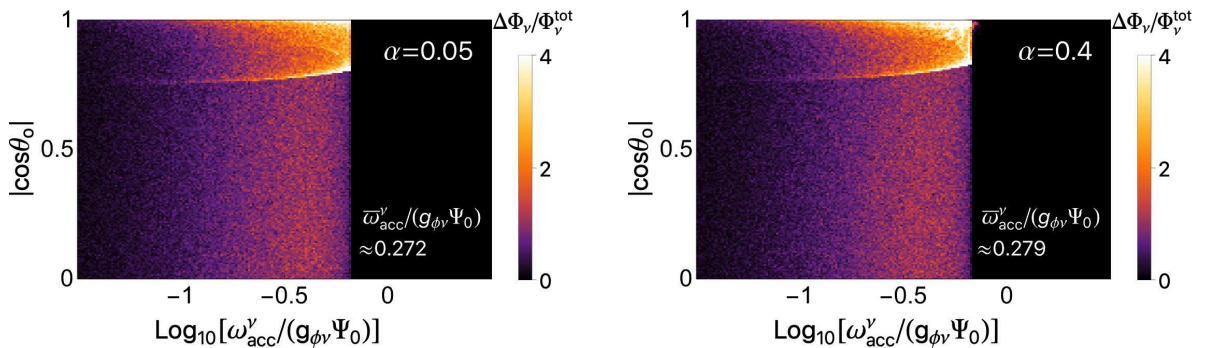

FIG. S1.   Same as Fig. 1 of the maintext with $\alpha = 0.05$ and 0.4.